

General Disclaimer

One or more of the Following Statements may affect this Document

- This document has been reproduced from the best copy furnished by the organizational source. It is being released in the interest of making available as much information as possible.
- This document may contain data, which exceeds the sheet parameters. It was furnished in this condition by the organizational source and is the best copy available.
- This document may contain tone-on-tone or color graphs, charts and/or pictures, which have been reproduced in black and white.
- This document is paginated as submitted by the original source.
- Portions of this document are not fully legible due to the historical nature of some of the material. However, it is the best reproduction available from the original submission.

**NASA TECHNICAL
MEMORANDUM**

NASA TM X-71762

NASA TM X-71762

(NASA-TM-X-71762) PRESSURE DISTRIBUTION IN
A CONVERGING-DIVERGING NOZZLE DURING
TWO-PHASE CHOKED FLOW OF SUBCOOLED NITROGEN
(NASA) 12 p HC \$3.25 CSCL 20D

N75-26306

Unclas
26642

G3/34

PRESSURE DISTRIBUTION IN A CONVERGING-
DIVERGING NOZZLE DURING TWO-PHASE
CHOKED FLOW OF SUBCOOLED NITROGEN

by Robert J. Simoneau
Lewis Research Center
Cleveland, Ohio 44135



TECHNICAL PAPER to be presented at
Winter Annual Meeting of the American
Society of Mechanical Engineers
Houston, Texas, November 30 - December 5, 1975

**PRESSURE DISTRIBUTION IN A CONVERGING-DIVERGING NOZZLE DURING
TWO-PHASE CHOKED FLOW OF SUBCOOLED NITROGEN**

by Robert J. Simoneau
NASA Lewis Research Center
Cleveland, Ohio 44135

ABSTRACT

Choked flow rates and axial pressure distributions were measured for subcooled nitrogen in a converging-diverging nozzle with a constant area section in the throat region. Stagnation pressures ranged from slightly above saturation to twice the thermodynamic critical pressure. Stagnation temperatures ranged from 0.75 to 1.03 times the thermodynamic critical temperature. The choking plane appears to be at the divergence end of the constant area throat section. At high stagnation pressures the fluid appears to stay liquid well into the constant area throat region; however, at near saturation stagnation pressures it appears that vaporization occurs at or before the entrance to the constant area throat region. The throat-to-stagnation pressure ratio data exhibits an anomalous flat region. This anomaly appears to be fundamentally related to the two-phase process and not merely to the present specific nozzle geometry. The fluid appears to be metastably all liquid below the saturation pressure. The data are compared to various flow models. No model adequately describes the whole range of the experiment.

NOMENCLATURE

A= Area, cm²
d= Diameter, cm
G= Mass flux, gm/cm²-sec
k= Slip ratio, u_g/u_l
P= Pressure, N/cm²
S= Entropy, J/gm-k
T= Temperature, K
u= Velocity, m/sec
v= Specific volume, cm³/gm
W= Flow rate, gm/sec
x= Quality
z= Nozzle axial distance (z=0 at point of divergence), cm

Subscripts

e= Exit plenum conditions
c= Thermodynamic critical conditions
e= Equilibrium conditions
g= Saturated vapor conditions
l= Saturated liquid conditions
m= Momentum
max= Maximum
o= Stagnation conditions
sat= Saturation conditions
t= Throat conditions
z= At nozzle axial location z

INTRODUCTION

The field of two-phase choked flow has been extensively explored in the past ten years. This work has been quite thoroughly surveyed by Hsu (1), Herry, Grolmes, and Fauske (2), and Smith (3). Only that work directly related to the present study will be cited herein. Most of the two-phase choked flow work has been motivated by analyses of the Loss of Coolant Accident, the so called design base accident of the nuclear power industry. In space research the motivation has been the safe storage and handling of liquid cryogenics. Space cryogenics are normally stored under high pressure, sometimes well above the thermodynamic critical pressure, and they are also frequently at a temperature high enough that during depressurization of the storage tank saturation conditions will occur. Interestingly a pressurized water reactor operating at 600 F and 2000-2200 psia (590 K and 1380-1520 N/cm²) is subcooled and is in the same reduced temperature and pressure range as many stored cryogenics, ($T_o/T_c=0.910$ and $P_o/P_c = 0.624$ to 0.686).

Curiously there has been very little experimental work with subcooled liquids. Herry and Fauske (4) were only able to cite a few references and most of these were very nearly saturated and were through orifices. At Lewis Research Center we have undertaken to run an extensive series of experiments covering a variety of flow geometries and a wide range of stagnation conditions:

$$0.75 < T_o/T_c < 1.03$$

$$P_{sat}/P_c < P_o/P_c < 2.0$$

Most of this work has already been reported (5-9). The present experiment focuses on converging-diverging nozzles. The data include axial pressure distribution in the nozzles. Extensive data tables from this experiment are available in reference 9. The present paper summarizes these data, analyzes them in terms of current theories, and examines the question of nonequilibrium.

FLOW MODELS

The analytic models presented in this paper can be found in references 1 to 4. Since the paper includes a comparison of these flow models to the data, the highlights will be repeated herein. The basic assumption throughout is that the flow can be described by the one-dimensional momentum equation, neglecting friction.

$$-AdP = d(u_L W_L + u_G W_G) \quad (1)$$

This can be readily manipulated to the form.

$$-1 = G \frac{d(v_m G)}{dP} \quad (2)$$

where

$$v_m = \left[\frac{xk + (1-x)}{k} \right] \left[xv_g + k(1-x)v_L \right] \quad (3)$$

Equation (2) can be integrated, subject to the condition that $G = 0$ when $P = P_0$, to yield

$$G^2 = -\frac{2}{v_m^2} \int_{P_0}^P v_m dP \quad (4)$$

Equation (4) is good throughout the flow field. By carrying out the differentiation in equation (2) and setting $dG/dP = 0$, the choked flow condition can be defined.

$$G_{\max}^2 = -\left. \frac{dv_m}{dP} \right|_t^{-1} \quad (5)$$

The point where choking occurs is designated the throat. The choked flow condition then is found by solving for the intersection of equation (4), which is valid throughout the flow field, and equation (5), which is valid only at the throat. The introduction of models is involved in attempting to define G and to evaluate dv_m/dP .

Of the models available for comparison, the homogeneous isentropic equilibrium model and the nonequilibrium model of Henry and Fauske (4) seemed most appropriate for initially subcooled flows. This choice is discussed in more detail in reference (9). Both models assume no slip, (i.e., $k=1$).

A departure in the present paper from previous computations is the use of exact thermodynamic properties throughout the flow field. In order to simplify calculations it has been very common to assume that the liquid properties are constant and that the vapor properties can be described by an ideal gas. This can be substantially in error if the stagnation conditions are well away from the saturation locus, especially if T_0 is near the thermodynamic critical temperature. In the present equilibrium model v_m is computed everywhere as a function of pressure and entropy, using a comprehensive property program, OASP (10).

It has long been believed that a degree of thermodynamic nonequilibrium exists in two-phase choked flow. Only Henry and Fauske (4), however, have attempted to formulate this belief into a practical model to describe the flow. There are three basic assumptions which describe the nonequilibrium character for an initially subcooled flow. First, it is assumed that no net vaporization occurs beyond the initial quality. Thus for subcooled flow the quality is assumed to be zero up to the throat. The second assumption is the one that really describes the particular nature of the nonequilibrium phenomenon. Henry and Fauske propose that, despite no net vapor generation up to the throat, there is at the throat a rate of change of quality and this can

be related to the equilibrium quality.

$$\left. \frac{dx}{dP} \right|_t = \begin{cases} \frac{x_e}{0.14} \left[\frac{dx}{dP} \right]_{t,e} & x_e < 0.14 \\ \left[\frac{dx}{dP} \right]_{t,e} & x_e \geq 0.14 \end{cases} \quad (6)$$

The final assumption is that the liquid specific volume, v_L , is treated as constant at the saturation value corresponding to the stagnation temperature. This assumption may not be valid for stagnation conditions well away from saturation and for stagnation temperatures above the thermodynamic critical temperature. Adjustments were made for this in the computations. This is discussed in the RESULTS section.

DESCRIPTION OF EXPERIMENT

The experiment was carried out in a "once-through" type cryogenic flow facility. The facility is illustrated schematically in figure 1. The essential elements include: a low pressure liquid nitrogen supply; a high pressure vessel; a nitrogen gas pressurizing system; an orifice flowmeter; the test section; a back pressure valve; a heat exchanger; and a second orifice flowmeter. In addition the high pressure nitrogen gas system was arranged so the gas could be used to warm the liquid. The pressure vessel, primary flowmeter and test section were enclosed in a vacuum envelope to minimize heat leaks. Fluid pressures and temperatures were measured at appropriate points in the flow system, as indicated. Mixing chambers formed the inlet and outlet plenums to the test section. The pressure and temperature measured in the inlet chamber were designated stagnation conditions. Choking was demonstrated by recording data at two different back pressure levels which had the same flow rate and throat to stagnation pressure ratio.

The test section used in this experiment, a conical converging-diverging nozzle, is shown in figure 2. It had a 7° half-angle convergence and a 3.5° half angle divergence. The small angles were used in an attempt to avoid separation and premature cavitation. The inlet to the throat was rounded to minimize cavitation. The outlet of the throat was sharp to distinctly mark the point of divergence. It had a constant area section at the throat with a length to diameter ratio of 3.20. The reason for a constant area section at the throat was to provide room for instrumentation. There were 15 pressure taps along the nozzle wall, mostly clustered near the constant area throat region. The interior surfaces were finished to 16 rms. For some of the tests the nozzle was turned around and used in the reverse orientation.

The only physical measurements made in this experiment were pressure and temperature. Pressures were all measured by the use of strain gage transducers. The fluid temperatures were measured throughout the flow system by use of platinum resistance thermometers. Two thermometers were located in each of the inlet and outlet mixing chambers. Flow rates were measured in two locations, as shown in figure 1. The primary meter was upstream and metered liquid flow. The backup flowmeter was located downstream of the test section, and the heat exchanger and consequently metered gas flow. Error

estimates based on the average over the range of the variable measured are presented in Table 1.

The data were recorded on a central data acquisition system and reduced at the test facility on a time-sharing computer. The thermophysical properties were computed using the computer sub-routine GASP (10).

RESULTS

Flow Rate and Pressure Ratio Data

The data taken in this experiment covered a wide range of stagnation parameters from a highly subcooled, very incompressible liquid to a compressible fluid above the thermodynamic critical point. In all cases the fluid expanded into the two-phase region. The experiment included the following stagnation conditions:

$$95 < T_0 < 130 \text{ K}$$

$$60 < P_0 < 660 \text{ N/cm}^2$$

$$10 < (P_0 - P_{\text{sat}}) < 600 \text{ N/cm}^2$$

The flow rate and pressure ratio data taken along 5 separate stagnation isotherms in the conically converging axisymmetric nozzle are plotted as a function of stagnation pressure in figure 3 and 4. Both the flow rate and the pressure ratio data exhibit anomalous behavior. The anomaly stands out more in the pressure ratio data, (fig. 4). It is definitely present, however, in the flow rate data, (fig. 3). In order to eliminate geometry effects the nozzle was turned around and the $T_0 = 110$ and 119 K isotherms were repeated with flow reversed through the nozzle. This changed the convergence and divergence angles and the approach to the constant area section. The results are presented in reference 9 and are in substantial agreement with figures 3 and 4. In addition, the data from a two-dimensional nozzle and another axisymmetric nozzle are presented in reference 9 to confirm that this behavior is not merely a special condition of a single nozzle. In the earlier experiments, (ref. 5), the flow rate anomaly was missed because it is small and there were not enough data points to delineate it.

As explained under FLOW MODELS the models selected for comparison of theory with the data were a homogeneous isentropic equilibrium model and the nonequilibrium model of Henry and Fauske (4). Henry-Fauske (4) assumed saturation conditions corresponded to the initial stagnation temperature, T_0 . Since in many of the cases the stagnation conditions are well away from the saturation locus, the question of the thermodynamic path to the saturation locus can be important. The difference in the value of the saturation pressure can easily be 50 N/cm^2 or more. Thus for the present comparison of theory to the data, the Henry-Fauske model was computed on both bases, the isothermal saturation pressure and the isentropic saturation pressure. In figures 3 and 4 the homogeneous equilibrium theory and the Henry-Fauske non-equilibrium theory are compared to the data from the conical axisymmetric nozzle.

The stagnation condition of $T_0 = 130 \text{ K}$ is above the thermodynamic critical temperature, ($T_c = 126.3 \text{ K}$). For all of the data along this isotherm the measured pressure and temperature in the exit plenum correspond to saturation conditions. This is the same as all the

other isotherms, and indicates the flow becomes two-phase somewhere in the nozzle. The measured throat pressure is at least 5 percent below the isentropic saturation pressure. The isentropic homogeneous equilibrium two-phase choked flow model predicts both the flow rate and pressure ratio data very well over the entire $T_0 = 130 \text{ K}$ isotherm as seen in figures 3 and 4. These results imply that two-phase choked flow can occur for stagnation temperatures above the thermodynamic critical temperature, and that the expansion path is isentropic. Because of the close correlation of the equilibrium theory to the data it would be tempting to conclude that the expansion was in thermodynamic equilibrium. However, at high stagnation pressures the throat pressure was consistently about 5 percent below saturation while the equilibrium model would predict the throat pressure to be the saturation pressure. While the close correlation of the data to the equilibrium theory is good for design purposes, it does not necessarily resolve the modeling question. On the other hand, the equilibrium model correctly predicts the existence of a peak in the pressure ratio curve and predicts its P_0 location to within 1.5 percent. The theory also predicts the rather rapid drop in pressure ratio followed by a leveling off as P_0 is further decreased. If the theory is correct, it suggests that the peak corresponds to the existence of wet quality at the throat and the leveling off occurs when the stagnation entropy exceeds the thermodynamic critical entropy. The final drop and leveling off occurs when the flow is no longer two phase. It seems clear that, although some non-equilibrium effects may persist, the two-phase expansion from $T_0 = 130 \text{ K}$ is very nearly in thermodynamic equilibrium.

The remaining isotherms are below the thermodynamic critical temperature. First, the reader is directed to the high pressure end of the spectrum. The Henry-Fauske model, using P_{sat}, T_0 , first over-predicts then under-predicts the flow rate as T_0 is increased. The theory always predicts a significantly higher pressure ratio than supported by the data. It should be pointed out that it is not possible to use P_{sat}, T_0 above the thermodynamic critical temperature, thus there is no theory curve for this model for the 130 K isotherm. Both the Henry-Fauske model, using P_{sat}, S_0 , and the isentropic homogeneous equilibrium model are more consistent with respect to the data. They both over-predict flow slightly and are quite close on pressure ratio. At the low stagnation pressures the equilibrium flow rates are as much as 30-50 percent below the data. The flow rate data agree well with the Henry-Fauske model at the low pressures. In fact, it can be said that over most of the entire range of the experiment the Henry-Fauske model, using P_{sat}, S_0 , predicts the choked flow rates consistently well, generally about 5-10 percent high.

This is not the case, however, with the pressure ratio. As the stagnation pressure decreases, the data and theory deviate significantly. All of the various models indicate a smooth variation of throat-to-stagnation pressure ratio as the stagnation pressure is varied along a given isotherm. The data indicate a clear anomalous flat spot and this is where the data and theory depart significantly. In the previous section it was pointed out that this behavior exists in all the nozzles tested and must be a physical phenomenon rather than the peculiarity of a certain test section. The data show that a high P_0

the throat pressure is approximately constant at a value near P_{sat, S_0} . At low P_0 the throat pressure is also nearly constant at a value well below saturation. In the region of the anomaly the throat pressure varies between these two limits. Also, while they are not as dramatic, the flow rates exhibit an anomaly and deviate from the trend of the theory curves. The effect can be as much as 25 percent.

Comparison To All Liquid Flow

In order to shed some light on this anomaly a calculation was performed which attempted to examine the influence of a metastable liquid. Ignoring the choking altogether the pressure drop was computed which for all liquid flow would yield the measured maximum flow rate (i.e., $AP = 0.5 \sqrt{\gamma} \sqrt{2 P_0}$). The pressure ratios resulting from this calculation are shown as solid symbols along with the pressure ratios at four nozzle stations in figure 5. Inspection of this figure indicates this calculation is significant. Looking first at the low stagnation pressure end, the slope is such that the pressure which corresponds to the measured flow is approximately constant ($P_0 = 180 \text{ N/cm}^2$), and is well below the isentropic saturation pressure (220-235 N/cm^2). At the high stagnation pressure end the pressure corresponding to measured flow is also constant near P_{sat, T_0} . The all liquid computation also yields an anomalous flat region in the middle, just as the actual data, in which the pressure ranges between these two constant limits. This result implies that in order to produce these high flow rates the fluid must remain liquid below the saturation pressure. It further implies that there is a limit in the pressure below saturation which can support a metastable liquid. It is important to point out here that this observation does not say that the fluid remains liquid all the way to the throat; or that the computed value is the metastable limit. In order to discuss this more fully it is necessary to examine the axial pressure profiles.

Axial Pressure Profiles

Before discussing the anomaly some general observations are in order. These are best made by comparing choked and unchoked flow pressure profiles. For each choked flow data point acquired, a complete pressure profile as a function of axial position was also recorded. Very little unchoked data were acquired. However, during the studies with the nozzle in the reversed flow orientation (see fig. 2), several sets of both choked and unchoked profiles were obtained for the same stagnation conditions in order to better define the choked flow pattern. These profiles are shown in figures 6 and 7. Both sets of profiles are nominally at 1 - 110 K. The data in figure 6 are at a relatively high stagnation pressure, $P_0 = 170 \text{ N/cm}^2$, and the data in figure 7 are at a relatively low stagnation pressure, $P_0 = 226 \text{ N/cm}^2$. The measure of this is the relative location of the saturation pressure.

The significant feature of the data in figure 6 is that the stagnation pressure is substantially above the saturation pressure. The average value of both the isothermal and isentropic saturation pressures are indicated on figure 6. The profiles in figure 6 are all remarkably similar up to the diverging end of the constant area, "throat,"

section. The first two profiles (readings 1331 and 1332) are clearly unchoked and all liquid, since the lowest pressure is 40 N/cm^2 above saturation. Readings 1333 and 1334 appear to be choked. The pressure drops in the constant area region are very similar in all four cases. This leads to the conclusion that the flow is all liquid to the exit end of the constant area region. The profiles in figure 7 present a different picture. The first reading, 1350, is very similar to the profiles in figure 6 and depending on which thermodynamic path is selected the constant area, "throat," pressures are either slightly above or slightly below the saturation pressure. The flow is not choked. The remaining three profiles are clearly different and in every case the pressures in the constant area region are clearly below saturation regardless of thermodynamic path. The profile for nitrogen gas is also shown on figure 7. In the constant area region the gas pressure distribution is very similar to that for these three profiles. This certainly seems to imply that vapor exists in the constant area region for all the nozzle profiles except the first, reading 1350. The combination of the data shown in figures 6 and 7 strongly implies that profiles which show a fairly steep pressure drop in the constant area section must be considered to have vapor present in the flow. Those profiles that almost level off in the constant area region appear to be all liquid to the point of divergence.

An additional question on which these profiles might offer some insight are the location of the choking plane or "throat." The first observation that can be made is that there must be vapor present for choking to occur. Thus for the flow situation of figure 6, where the fluid appears to be liquid throughout the constant area section, choking must occur at or near the point of divergence in the nozzle. For those conditions which indicate vapor in the constant area region, figure 7, substantial changes in downstream pressures produce minimal changes in the constant area region. It would appear that the choking plane is always at or near the exit to the constant region.

With this background we can return to the discussion of the anomaly. Figures 8-10 are axial pressure distributions in the nozzle for 3 data regions on figure 5. The reverse flow profile data were used to stay consistent with figures 6 and 7. Figure 8 represents the low stagnation pressure end of the spectrum where the throat pressure was found to be constant at a value well below saturation. It can be seen from figure 8 that several pressures upstream of the throat are below saturation. The pressure distribution in the constant area region suggests vapor is present at the entrance to or upstream of this section. On the other hand, an assumption of thermodynamic equilibrium evaporation when $P_0 = P_{sat, S_0}$ under predicts flow by 30 percent. The all liquid flow pressure is plotted as a solid symbol for reference. Figure 9 is in the anomalous flat region of figure 5 and the profile shape is very similar to figure 8 except that the throat pressure is nearer saturation. Equilibrium analysis underpredicts by 9 percent. The equilibrium flow rate discrepancy in both these cases suggests the flow must remain liquid below saturation which agrees with the interpretation of the all-liquid computation. The profiles indicate vaporization must occur at or before the throat entrance. Figure 10 corresponds to a high stagnation pressure and yields different results. The profile shape appears

all liquid to the exit of the constant area region. However, the all liquid computation (solid symbol) indicates the throat pressure is too low. Said another way, the equilibrium calculation overpredicts flow by 5 percent. A possible explanation is that the fluid remains liquid below P_{sat, S_0} and into the constant area region as suggested by the data of figure 10; but that when it vaporizes the small amount of vapor reduces the flow cross section. In terms of model formation the evidence suggests that the flow always remains liquid below P_{sat, S_0} but that it can vaporize before the throat. The model appears subject to the thermodynamic region of the stagnation condition and it is not as simple as previously proposed. Finally, it should be noted that only the 110 and 119 K isotherms exhibit all three regions. A complete discussion of all isotherms is beyond the limitations of this paper and is taken up in reference 9.

CONCLUSIONS

A two-phase choked flow experiment was conducted using subcooled liquid nitrogen, flowing in a converging-diverging nozzle with a constant area section in the throat region. The experiment covered a range of inlet stagnation temperatures from 0.75 to 1.03 times the thermodynamic critical temperature and inlet stagnation pressures from slightly above saturation to twice the thermodynamic critical pressure. The data of the experiment include the axial pressure distribution at fifteen stations along the nozzle. While the conclusions from these data are only directly applicable to nitrogen over the stated range, it is the opinion of the author that they are applicable to other fluids, especially simple cryogenics, over similar reduced pressure and temperature ranges. The choked flow rate and pressure distribution data, along with comparisons to various theories, lead to several conclusions.

1 Under some choked flow circumstances the flow can be all liquid into the constant area throat region and under other circumstances vaporization occurs at or before the entrance to the constant area region.

2 The choking plane or "throat" is always at or near the point of divergence from the constant area region in the nozzle.

3 The data of this experiment show a strong anomalous flat region in the pressure ratio data. This anomaly appears in the flow rate data as well. It occurs in other nozzles tested and appears to be fundamentally related to the two-phase process.

4 The data were compared to the homogeneous equilibrium theory and to the nonequilibrium theory of Henry and Fauske. At stagnation temperatures below the thermodynamic critical temperature no theory completely describes the phenomena, especially the anomaly cited. However, the nonequilibrium theory of Henry and Fauske, using an isentropic path to the saturation locus best describes the flow rates. It is consistently about 5-10 percent high, except in the anomalous region.

5 For the stagnation isotherm above the thermodynamic critical temperature the is.ropic homogeneous equilibrium model describes the flow rate and pressure ratio very well. The fact that

the computed pressure ratio is consistently about 5 percent high suggests that maybe a small non-equilibrium effect may persist into this region.

6 Pressure ratios computed from the flow rates on the assumption of all liquid flow follow exactly the trends in the pressure ratio data, including the anomalous flat region. An analysis of this result leads to the conclusion that there does exist thermodynamic nonequilibrium whereby the fluid does not vaporize immediately upon crossing the saturation pressure locus. There does, however, appear to be a lower limit in pressure that cannot be exceeded without vaporization. Also, vaporization can occur ahead of the throat. The model for this nonequilibrium phenomenon is not as simple as proposed by Henry and Fauske. It seems to be a function of the thermodynamic region of the stagnation conditions.

REFERENCES

- 1 Hsu, Y. Y., "Review of Critical Flow, Propagation of Pressure Pulse and Sonic Velocity," NASA TN D-6814, 1972.
- 2 Henry, R. E., Grolmes, M. A., and Fauske, H. K. "Pressure Drop and Compressible Flow of Cryogenic Liquid-Vapor Mixtures," Heat Transfer at Low Temperatures, W. Frost, ed., Plenum Press, New York, 1975, pp. 229-259.
- 3 Smith, R. V., "Critical Two-Phase Flow for Cryogenic Fluids," NBS Tech Note 633, Jan. 1973.
- 4 Henry, R. E., and Fauske, H. K., "The Two-Phase Critical Flow of One-Component Mixtures in Nozzles, Orifices, and Short Tubes," Journal of Heat Transfer, Vol. 93, No. 2, May 1971, pp. 179-187.
- 5 Hendricks, R. C., Simoneau, R. J., and Eilers, R. C., "Choked Flow of Fluid Nitrogen with Emphasis on the Thermodynamic Critical Region," Advances in Cryogenic Engineering, Vol. 18, Timmerhaus, K. D., ed., Plenum Press, New York, 1973, pp. 150-161.
- 6 Simoneau, R. J., "Two-Phase Choked Flow of Subcooled Nitrogen Through a Slit," Proceedings of the Tenth Southeastern Seminar on Thermal Science, Watts, R. G., and Sogin, H. H., ed., New Orleans, Louisiana, 1974, pp. 225-238.
- 7 Hendricks, R. C., "Normalizing Parameters for the Critical Flow Rate of Simple Fluids Through Nozzles," Proceedings of the Fifth International Cryogenic Engineering Conference, Kyoto, Japan, May 1974.
- 8 Simoneau, R. J., "Maximum Two-Phase Flow Rates of Subcooled Nitrogen Through a Sharp-Edged Orifice," To be presented at the 1975 Cryogenic Engineering Conference, Kingston, Ontario, Jul. 1975.
- 9 Simoneau, R. J., "Two-Phase Choked Flow of Subcooled Nitrogen in Converging-Diverging Nozzles," NASA TN to be published.
- 10 Hendricks, R. C., Baron, A. K., and Peller, I. C., "GASP-A Computer Code for Calculating the Thermodynamic and Transport Properties for Ten Fluids: Parahydrogen, Helium, Neon, Methane, Nitrogen, Carbon Monoxide, Oxygen, Fluorine, Argon, and Carbon Dioxide." NASA TN D-7808, Feb. 1975

TABLE 1

Error Estimate for the Parameters Measured in This Experiment

Parameter		Range	Error Estimate Percent of Average Value	Error Estimate Absolute
Pressures:				
Stagnation	P_0	60 - 680 N/cm ²	<u>+0.4</u>	+1.4 N/cm ²
Throat	P_t	33 - 275 N/cm ²	<u>+0.9</u>	
Back	P_b	20 - 100 N/cm ²	<u>+2.3</u>	
Axial	P	30 - 550 N/cm ²	<u>+0.5</u>	
Temperatures:				
Stagnation	T_0	90 - 130 K	<u>+0.1</u>	<u>+0.1 K</u>
Back	T_b	84 - 104 K	<u>+0.1</u>	<u>+0.1 K</u>
Mass Flux: G				
	(95 - 125 K isotherms)	1600 - 9000 gm/cm ² sec	<u>+1.4</u>	<u>+75 gm/cm² sec</u>
	(130 K isotherm)	1700 - 6000 gm/cm ² sec	<u>+2.1</u>	<u>+80 gm/cm² sec</u>

E-8415

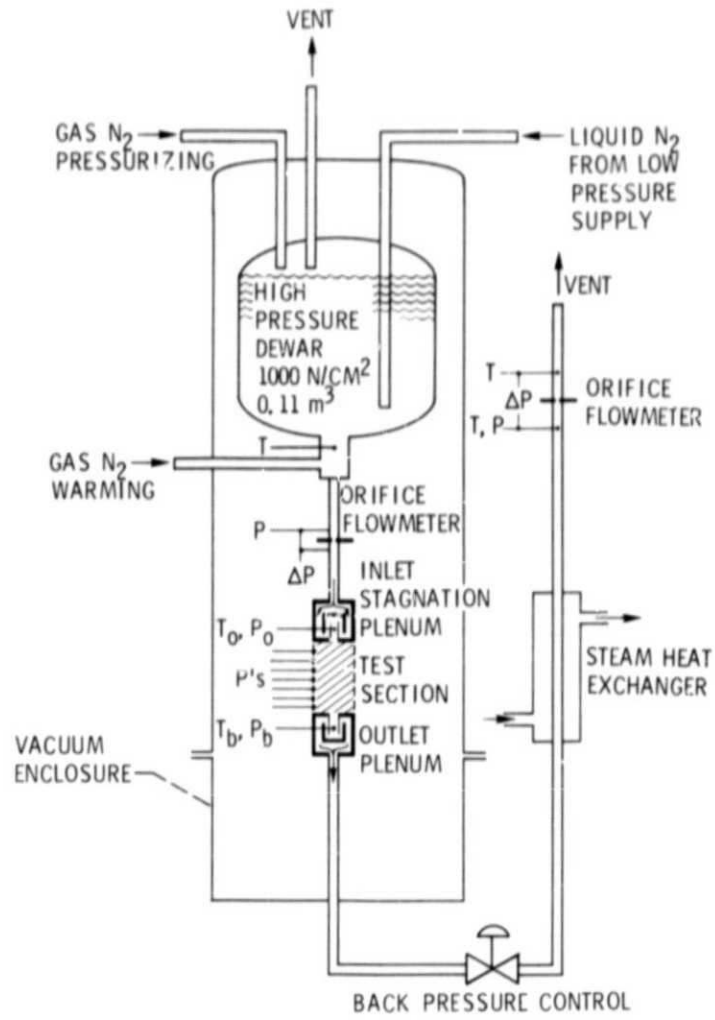
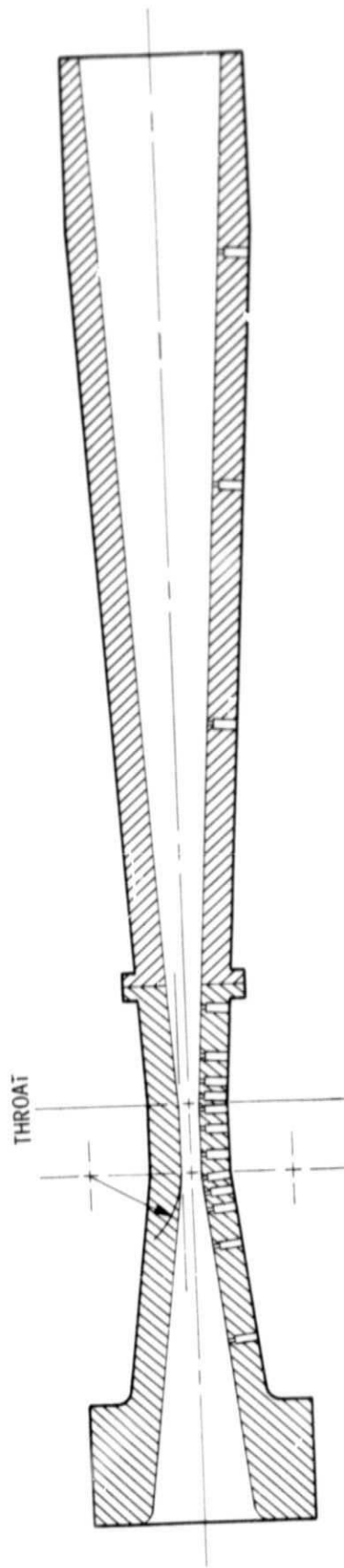


Figure 1. - Flow system schematic.



THROAT AREA = 0.0993 CM²

Figure 2. - Axisymmetric converging - diverging nozzle with conical convergence at 7° half angle and divergence at $3\frac{1}{2}^{\circ}$ half angle.

E-8415

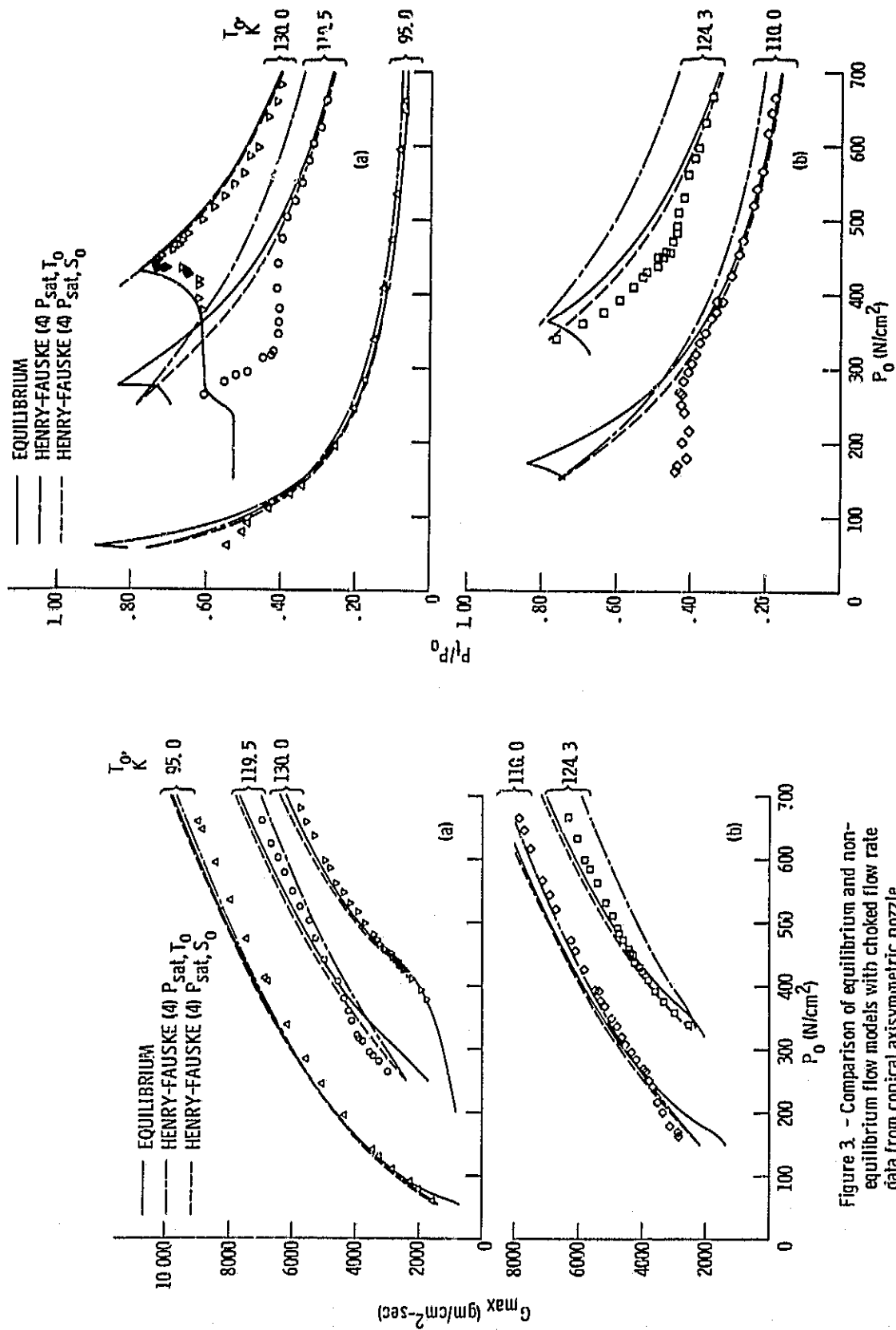


Figure 3 - Comparison of equilibrium and non-equilibrium flow models with choked flow rate data from conical axisymmetric nozzle.

Figure 4 - Comparison of equilibrium and non-equilibrium flow models for throat-to-stagnation pressure ratio during choked flow in conical axisymmetric nozzle.

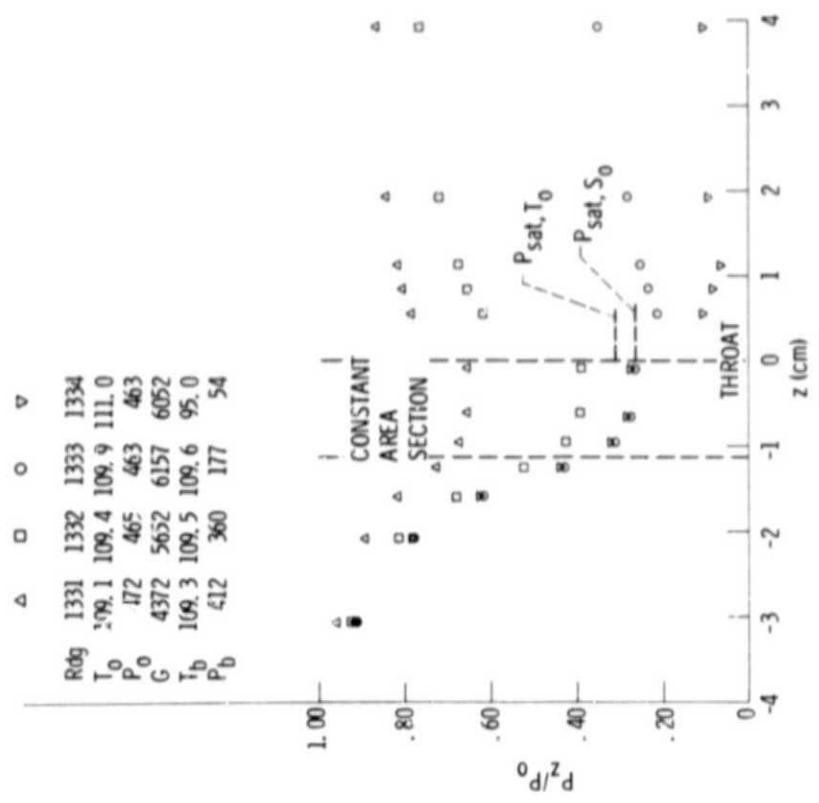


Figure 6. - Choked and unchoked pressure profiles in axisymmetric nozzle in reverse flow. $T_0 = 110 \text{ K}$, $P_0 = 470 \text{ N/cm}^2$.

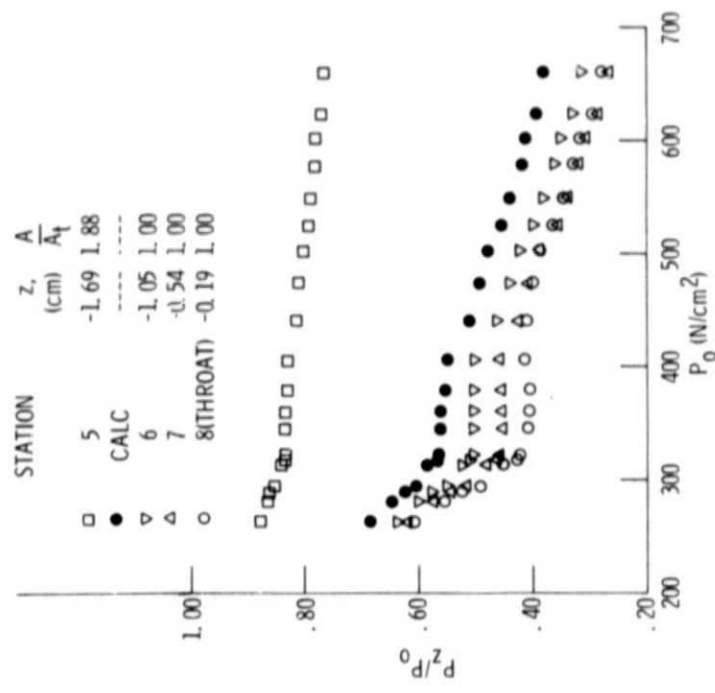


Figure 5. - Pressure ratios at various stations in conical axisymmetric nozzle compared to that calculated from maximum flow rate. $T_0 = 119.3 \text{ K}$.

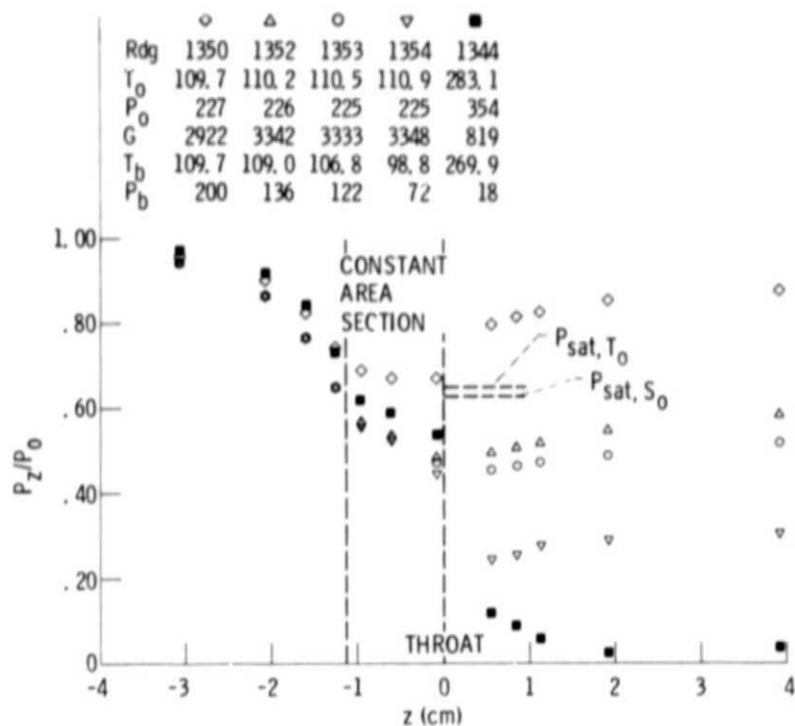


Figure 7. - Choked and unchoked pressure profiles in axisymmetric nozzle in reverse flow. $T_0 = 110$ K, $P_0 = 226$ N/cm²

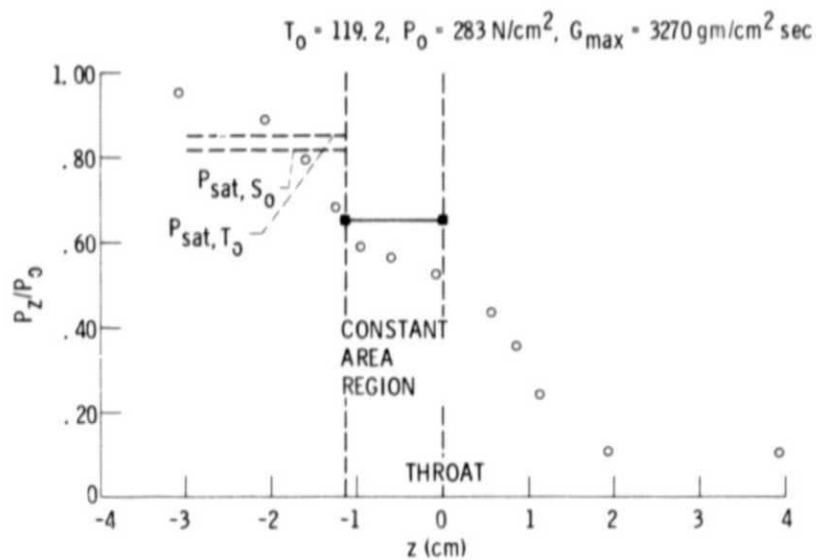


Figure 8. - Axial pressure distribution during choked flow in axisymmetric nozzle in reverse flow.

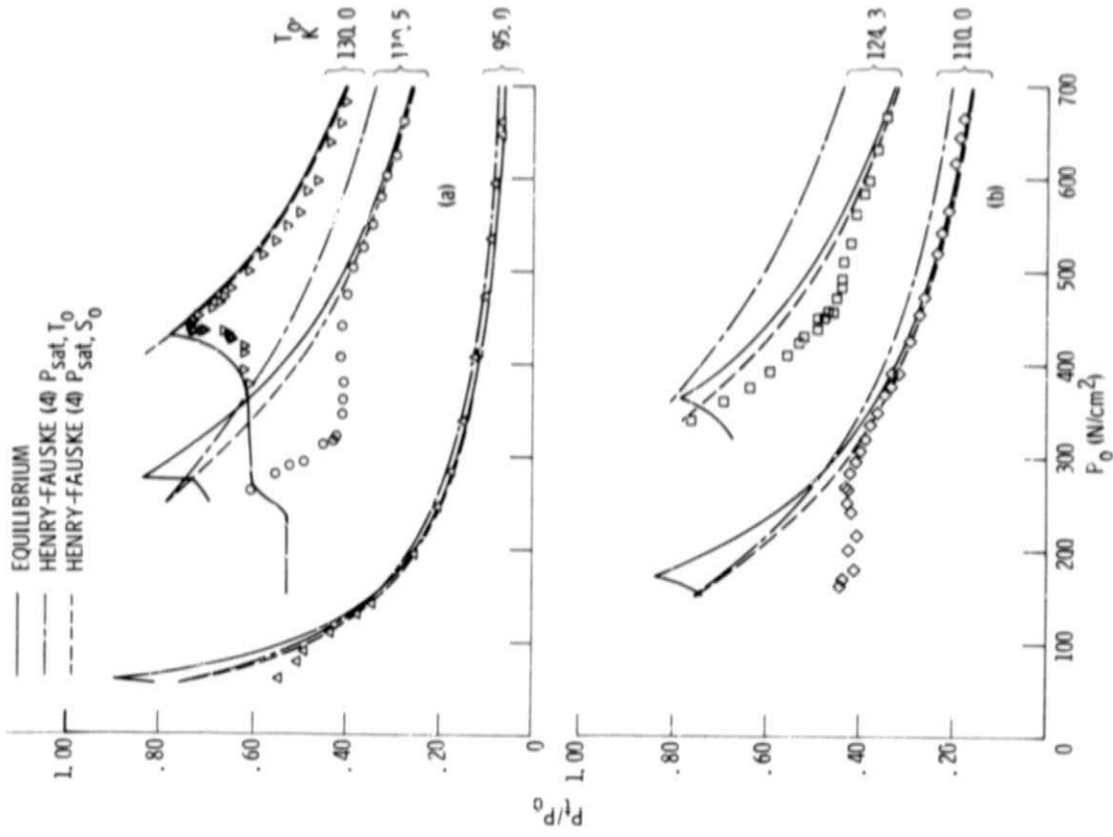


Figure 3. - Comparison of equilibrium and non-equilibrium flow models with choked flow rate data from conical axisymmetric nozzle.

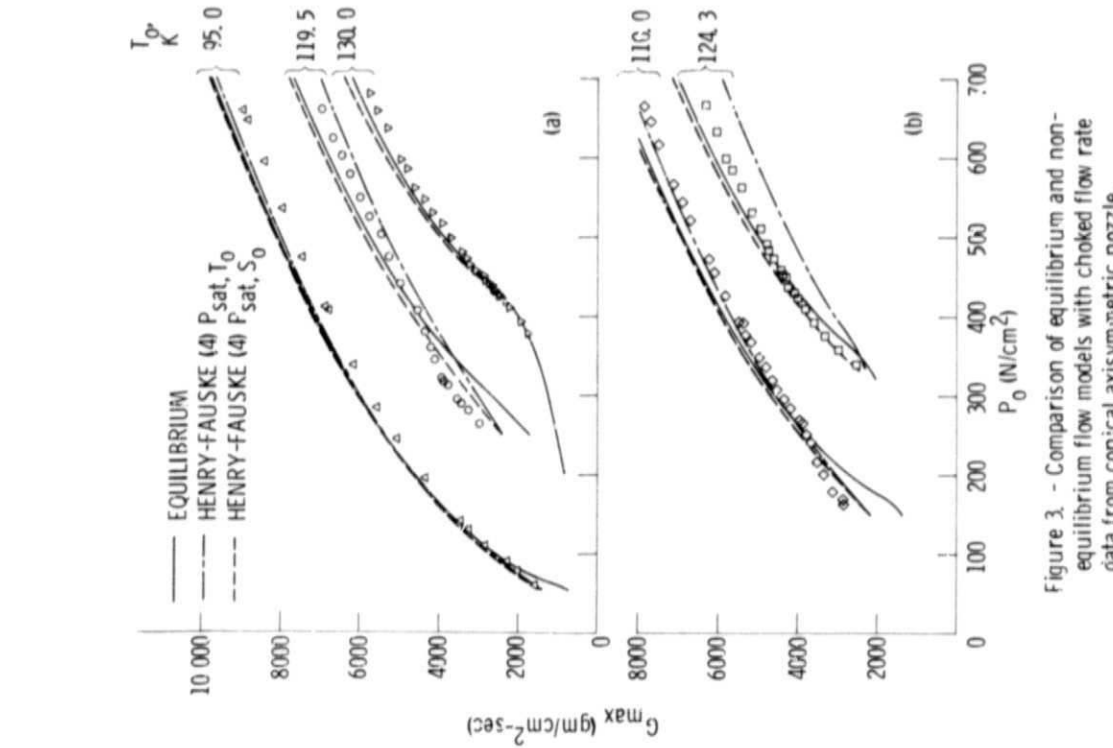


Figure 4. - Comparison of equilibrium and non-equilibrium flow models for throat-to-stagnation pressure ratio during choked flow in conical axisymmetric nozzle.

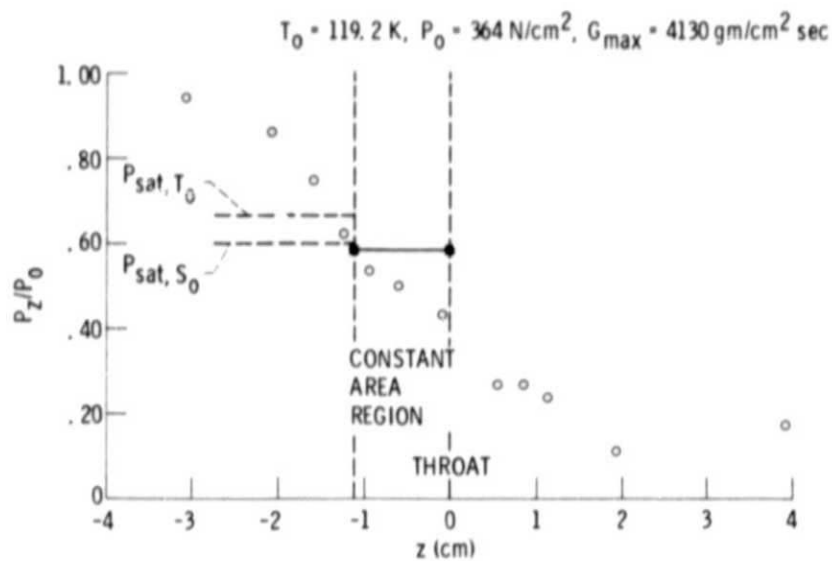


Figure 9. - Axial pressure distribution during choked flow in axisymmetric nozzle in reverse flow.

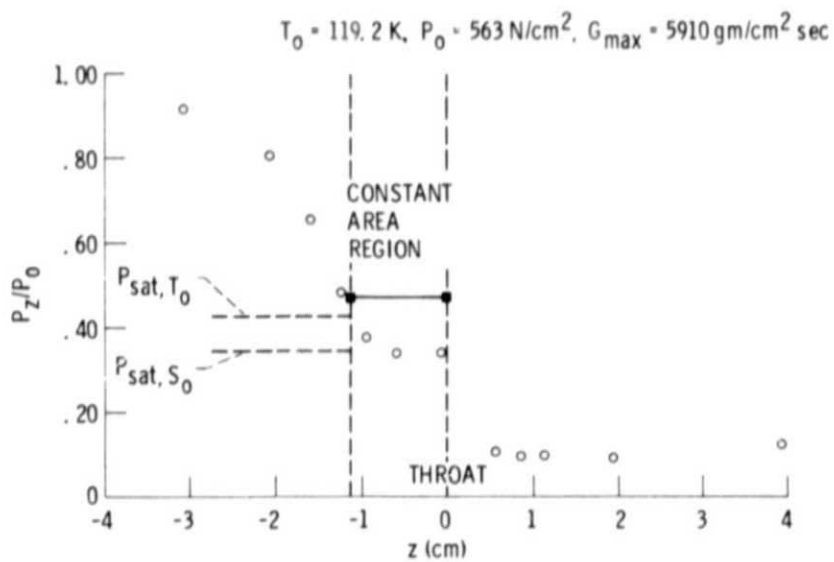


Figure 10. - Axial pressure distribution during choked flow in axisymmetric nozzle in reverse flow.